Phase Behavior of Stratum Corneum Lipid Mixtures Based on Human Ceramides: The Role of Natural and Synthetic Ceramide 1

Joke A. Bouwstra,* Gert S. Gooris,* Frank E. R. Dubbelaar,* and Maja Ponec†

*Leiden/Amsterdam Center for Drug Research, Gorlaeus Laboratories, Leiden University, Leiden, The Netherlands; †Department of Dermatology, Leiden University Medical Center, Leiden, The Netherlands

In a recent study the lipid phase behavior of mixtures of human ceramides, cholesterol, and free fatty acids has been examined. We observed in cholesterol: human ceramide mixtures a prominent formation of the 12.8 nm lamellar phase (referred to as the long periodicity phase). Addition of free fatty acids promoted the formation of a 5.6 nm lamellar phase (referred to as the short periodicity phase) and increased the subpopulation of lipids forming a fluid phase. In this study we focused on the role of human ceramide 1, as the presence of this ceramide appeared to be crucial for proper lipid phase behavior in mixtures prepared with ceramide isolated from pig stratum corneum. In order to do this, mixtures of cholesterol and free fatty acids were prepared with human ceramides, in which natural human ceramide 1 was replaced by either synthetic CER1-linoleate (CER1-lin), or CER1-oleate (CER1-ol), or CER1-stearate (CER1-ste). After substitution of natural human ceramide 1 by synthetic ceramide 1 the following observations were made. (i) In the presence of synthetic CER1-ste no long periodicity phase and no liquid phase could be detected. (ii) In the presence of HCER1-ol a liquid phase was more prominently formed than in the presence of HCER1-lin. (iii) In cholesterol:human ceramide mixtures in the presence of CER1-lin the long periodicity phase was more prominently present than in the presence of CER1-ol. (iv) In the presence of CER1-ste neither a long periodicity phase nor a liquid lateral packing could be detected. The results of these studies further indicate that for the formation of the long periodicity phase a certain (optimal) fraction of lipids has to form a liquid phase. When the fraction forming this liquid phase is either too low or too high, the formation of the short periodicity phase is increased at the expense of the formation of the long periodicity phase. Based on the results of this and previous studies we offer an explanation for the deviation in lipid organization in diseased and in dry skin compared to normal skin.

Key words: human ceramide 1/lipids/phase behavior/X-ray diffraction. J Invest Dermatol 118:606–617, 2002

It has been known for many years that the stratum corneum (SC) is of great importance for proper skin barrier function. As the lipid-rich intercellular regions in the SC are the only continuous domains, these lipid domains play a prominent role in the skin barrier function. For this reason the SC lipid composition and organization have been extensively studied over the last 20 y. Using electron microscopy it has been established that the SC lipids are organized in lamellar sheets (Madison *et al*, 1987) oriented approximately parallel to the corneocyte surface. These lipid lamellae have an unusual repeating pattern consisting of a broad–narrow–broad sequence of electron-lucent bands. In SC nonpolar lipid classes such as ceramides (CER), cholesterol (CHOL) and long chain free fatty acids (FFA) dominate. This exceptional lipid composition results in the predominant formation of a crystalline sublattice in the lamellar sheets as established by bulk methods such as Fourier transformed infrared spectroscopy (Gay *et al*, 1994) and X-ray diffraction (White *et al*, 1988; Bouwstra *et al*, 1991). More recently these results have been confirmed by methods that provide information on local lipid organization, such as atomic force microscopy (Chien and Wiedmann, 1996) and electron diffraction (Pilgram *et al*, 1999).

In previous studies X-ray diffraction experiments revealed that in pig, human, and mouse SC a lipid lamellar phase with periodicity of approximately 13 nm (referred to as the long periodicity phase, LPP) is present. In addition in human and pig SC a second lamellar phase with a periodicity of only 6 nm (referred to as the short periodicity phase, SPP) is present (White *et al*, 1988; Bouwstra *et al*, 1991, 1994, 1995). Furthermore, in mouse and human SC the lipids are predominantly organized in an orthorhombic lateral sublattice (White *et al*, 1988; Garson *et al*, 1991; Bouwstra *et al*, 1992, 1994), whereas in pig SC the lipids are in a hexagonal sublattice (Bouwstra *et al*, 1995). As the 13 nm phase is present in all examined species and is of an unusual lipid arrangement (Swartzendruber, 1992; Bouwstra *et al*, 1998a), this phase has been considered to be very important for the permeability barrier of the skin.

Manuscript received March 22, 2001; revised June 27, 2001; accepted for publication July 2, 2001.

Reprint requests to: Dr. J.A. Bouwstra, Leiden/Amsterdam Center for Drug Research, Gorlaeus Laboratories, Leiden University, PO Box 9502, 2300 RA Leiden, The Netherlands. Email: Bouwstra@chem.leidenuniv.nl

Abbreviations: CER, ceramide; CHOL, cholesterol; *d*, periodicity of lamellar phase; FFA, free fatty acids; LPP, long periodicity phase; *Q*, scattering vector; SC, stratum corneum; SPP, short periodicity phase; θ, scattering angle.

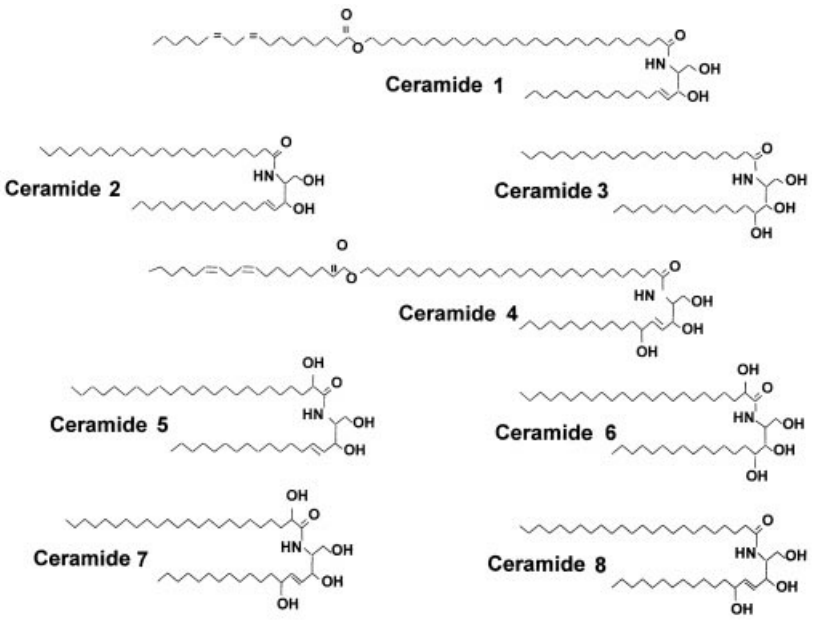

Figure 1. The molecular architecture of human CERs.

Information on the relationship between lipid organization and composition is of great importance to unravel the mechanisms controlling the skin barrier function. This is particularly demonstrated in diseased skin, in which an impaired barrier function can often be ascribed to an altered lipid composition and organization. For example, in lamellar ichthyosis skin the FFA content is strongly reduced (Lavrijsen *et al*, 1995) whereas in X-linked ichthyosis skin cholesterol sulfate level is increased (Elias *et al*, 1984). Examples of an altered CER content have been reported as well. In psoriatic, atopic dermatitis (Imokawa *et al*, 1991; Di Nardo *et al*, 1998) and dry skin (Schreiner *et al*, 2000) a decreased ceramide 1 (CER1) level has been found, whereas in essential fatty acid deficient skin (Melton *et al*, 1987) and skin with winter xerosis the balance between CER1-linoleate/CER1-oleate has been strongly disturbed (Conti *et al*, 1996). Until now, however, only limited information is available about the relation between SC lipid composition and organization. As it is impossible to extract the lipids selectively from the SC and the availability of diseased skin is very low, it is not possible to investigate systematically the role the various lipid classes play in the lipid organization with native SC. A systematic study can be performed, however, with lipid mixtures prepared from isolated SC lipids. Recently, the lipid organization of mixtures prepared with CER isolated from pig SC (pigCER) has been examined with the X-ray diffraction technique. We chose pigCER because it is readily available and the lipid organization in pig SC is similar to that in human SC. These studies revealed that when isolated pigCER are mixed with CHOL, two lamellar phases are formed with periodicities of 5.2 and 12.2 nm, respectively, that mimic the lipid organization in intact pig SC (Bouwstra *et al*, 1996). Addition of long chain FFA increased the periodicities of the lamellar phases slightly and induced a phase transition from a hexagonal sublattice to an orthorhombic one (Bouwstra *et al*, 1998b), in this way increasing the density of the structure. An additional study in which the effect of pigCER composition on lipid organization was examined revealed that the phase behavior of equimolar mixtures was rather insensitive towards a change in CER composition with one exception. In the absence of pigCER1, the intensity of the peaks attributed to the LPP was dramatically reduced, demonstrating the importance of CER1 for the lipid organization in the SC (McIntosh *et al*, 1996; Bouwstra *et al*, 1998a).

CER isolated from pig SC (Wertz and Downing, 1983) differ in molecular architecture from CER isolated from human SC (HCER) (see **Fig 1**, Robson *et al*, 1994). Human ceramide 1 (HCER1) and human ceramide 4 (HCER4) both have a very exceptional molecular structure: a linoleic acid is linked to an ω-hydroxy acid with a chain length of approximately 30–32 C-atoms. In this respect the HCER differ from pigCER, in which only CER1 has this exceptional molecular structure. For this reason the studies on the role the lipid classes play in the phase behavior of mixtures based on HCER can help us to understand in more detail the mechanisms leading to changes in barrier function and lipid organization in diseased and dry skin. Even in normal skin, seasonal changes in lipid composition have been noticed (Conti *et al*, 1996); the ratio of CER linoleate to CER oleate showed a dramatic change from 1.74 to 0.51 from the summer to the winter months. Therefore, in this study we have focused on the role HCER1 plays in the SC lipid phase behavior. To achieve this the phase behavior was examined in CHOL:HCER mixtures in which the natural HCER1 was replaced by either synthetic CER1 linoleate (CER1-lin), synthetic CER1 oleate (CER1-ol), or synthetic CER1 stearate (CER1-ste).

MATERIAL AND METHODS

Extraction, separation, and identification of lipids from SC Human abdomen or breast skin was obtained after cosmetic surgery and processed on the same day. The subcutaneous fat was removed and the skin was dermatomed to a thickness of approximately 250–300 μm (Padgett Dermatome, Kansas City, KS). To isolate the SC, the dermatomed skin was incubated with its dermal side placed on a Whatman paper soaked in a solution of 0.1% (wt/vol) trypsin (Sigma, Zwijndrecht, The Netherlands) in 0.15 M phosphate-buffered saline (PBS) (NaCl 8 g per liter, KCl 0.19 g per liter, KH_2PO_4 0.2 g per liter, Na_2HPO_4) and incubated overnight at 4°C followed by 1 h at 37°C. After this the SC was peeled off from the epidermis and dermis. SC lipids were extracted using the method of Bligh and Dyer (1959). The extracted lipids were applied on a silica gel 60 (Merck) column with a diameter of 2 cm and a length of 33 cm. The various lipid classes were eluted sequentially using various solvent mixtures as published recently (Bouwstra *et al*, 1996). The lipid composition of collected fractions was established by one-dimensional high performance thin layer chromatography, as described earlier (Ponec *et al*, 1988). For quantification, CER3 obtained from Cosmoferm was run in parallel. The quantification was performed after charring using a photodensitometer (Biorad, GS 710). Isolated HCER fractions were mixed to achieve a composition similar to that in intact human SC.

Preparation of lipid mixtures Various classes of lipids were mixed in various molar ratios, using a mean HCER molar weight of 700. Mixtures were prepared from either CHOL and HCER or CHOL,

HCER, and FFA. In these studies the following HCER mixtures were prepared, in which natural HCER1 is replaced by synthetic CER1-linoleate (HCER1-lin, 2–8), or synthetic CER1-oleate (HCER1-ol, 2–8), or synthetic CER1-stearate (HCER1-ste, 2–8). The ω-hydroxy acyl chain length of the synthetic CER is C27; the sphingosine chain is C22. The synthetic CER1 were provided by Unilever Research.

For the FFA we chose a mixture of long chain FFA with a similar composition to that in SC (Wertz and Downing, 1991). The fatty acid composition was C16:0, C18:0, C22:0, C24:0, and C26:0 in a molar ratio 1:3:42:37:7. A detailed description of the lipid mixture preparation is given elsewhere (Bouwstra *et al*, 1996). Briefly, approximately 2 mg of lipids at the desired composition were solubilized in chloroform:methanol (2:1) and applied on mica. The organic solvent was evaporated under a stream of nitrogen, after which the sample was heated to 60°C. After 10 min of equilibration the lipid mixtures were covered with 1–2 ml buffer at pH 5.0, and cooled down. Then at least 10 freeze–thawing cycles were carried out. The mixtures were prepared at either pH 5, which is the approximate pH at the skin surface, or pH 7.4, the pH at the SC–stratum granulosum interface (Aly *et al*, 1978; Sage *et al*, 1993; Ohman and Vahlquist, 1994). To achieve a pH of 5 an acetate buffer (10 mmol, Na^+ based) was used; to prepare mixtures at a pH of 7.4 a HEPES buffer (10 mmol, Na^+ based) was used.

Diffraction methods

Explanation of the X-ray diffraction methods In the case of X-ray diffraction, a source produces X-rays, of which a small part are scattered by the sample. The scattered intensities are measured as a function of $\theta/2$, the scattering angle (see **Fig 2*A***). When the sample consists of a regular structure with a repeating pattern, the intensity of the scattered X-rays in the diffraction pattern is characterized by a series of peaks (intensity maxima of scattered X-rays). Often, the scattered intensity is plotted as a function of Q (the scattering vector), which is directly related to the scattering angle by $Q = 4\pi \sin(\theta)/\lambda$, in which λ is the wavelength of the X-rays. In case of small angle X-ray diffraction the scattered intensity is measured at low angle, typically between 0 and 5°. From the diffraction pattern, information can be obtained about the larger structural units in the sample, such as the repeat distance of a lamellar phase (see **Fig 2*B***). Wide angle X-ray diffraction provides information about the scattered intensity at higher angle (see **Fig 2*A***). From the diffraction pattern obtained at higher angle, X-ray information about the smaller structural units in the sample can be acquired, such as the lateral packing in a lamellar phase (see **Fig 2*B***).

Small angle X-ray diffraction The X-ray diffraction pattern of a lamellar phase is characterized by a series of peaks, of which the sequential peaks are positioned at equal interpeak distance. The position of the sequential peaks is referred to as first order (positioned at Q_1), second order (Q_2), third order (Q_3), etc. The repeat distance (d_A) of a lamellar phase A can be directly calculated from the peak positions: $d_A = 2\pi/Q_1 = 4\pi/Q_2 = 6\pi/Q_3$, etc. A larger repeat distance in the structure results in a series of peaks with a smaller interpeak distance at the scattered X-ray curve (compare d_A and d_B in **Fig 2*B***).

When two lamellar phases are present in the sample (lamellar phases A and B with repeat distances d_A and d_B) the scattered X-rays are additive.

Wide angle X-ray diffraction Wide angle X-ray diffraction provides information about the localization of the lipids in the lamellae. For SC lipid organization three classes of lateral packing are important. In the liquid phase the distance between the molecules is not well defined, which results in an X-ray pattern with a very broad peak at around 0.46 nm. This phase is highly permeable. In hexagonal lateral packing, which is a much denser structure than the liquid one, the distance between neighboring molecules in the x–y plane is equal. The diffraction pattern of this packing is characterized by one strong reflection at approximately 0.41 nm spacing. Finally, the orthorhombic phase is a very densely packed structure with very low permeability. The neighboring molecular distance in the x and y directions is not equal and two strong diffraction reflections at 0.37 and 0.41 nm spacing can be detected. The relation between lateral packing and the diffraction pattern is given schematically in **Fig 2(*C*)**.

Small angle X-ray diffraction All measurements were carried out at the Synchrotron Radiation Source at Daresbury Laboratory using station 8.2. The samples were placed in a specially designed sample holder with two mica windows. A detailed description of the equipment has been given elsewhere (Bouwstra *et al*, 1991). The experimental conditions were similar to those described in a previous publication (Bouwstra *et al*, 2001). The scattered intensities were measured as a function of θ, the scattering angle. Calibration of the detector was carried out with rat tail and CHOL. From the scattering angle the scattering vector (Q) was calculated. The wavelength at the sample position was 0.154 nm.

The intensities of the various diffraction curves of the samples were scaled using the tail of the diffraction curve.

Wide angle X-ray diffraction The diffraction patterns were obtained at room temperature with a fiber diffraction camera at station 7.2 of the synchrotron radiation source in Daresbury. A more detailed description of the equipment is given elsewhere (Bouwstra *et al*, 1992). A description of the method has been provided in a previous publication (Bouwstra *et al*, 2001).

Calculation of peak intensities As the amount of lipids in the X-ray beam differ in each experiment, calculation of the absolute amounts of lipids forming a particular phase in the mixture exposed to the X-rays makes no sense. An indication about the presence of a particular phase, however, can be obtained from the ratio between the intensities of selected peaks attributed to different phases. In this study we are interested in whether lipid composition affects the formation of the liquid lateral packing. Evidence about the presence of the liquid lateral packing can be obtained from the ratio between the intensities of the 0.46 nm peak (liquid phase) and either the 0.406 nm peak (hexagonal lattice) or the 0.406 + 0.367 nm peaks (orthorhombic lattice). An increase in the liquid:crystalline peak intensity ratio indicates an increase in the fraction of lipids forming the liquid phase. In making this correlation we assume that the relative intensity of the various peaks attributed to the same phase is constant irrespective of a small change in lipid composition. As in this study peaks attributed to CHOL sometimes obscure the peak attributed to the liquid phase, we first subtract the peaks attributed to crystalline CHOL from the diffraction curve. This is carried out with the known diffraction profile of hydrated crystalline CHOL. Then we calculate the areas of the selected peaks by assuming a Gaussian distribution of the intensity. Evidence for the presence of the LPP can be obtained from the second and third order peaks of the LPP and the first order peak of the SPP. A more prominent presence of the LPP is indicated by an increase in the intensity ratio of second + third order diffraction peaks of the LPP and the first order diffraction peak of the SPP. Peak areas are again calculated by fitting the intensities assuming a Gaussian distribution.

RESULTS

Lipid composition The CER composition as determined by high performance thin layer chromatography is 9.4% (HCER1), 31.7% (HCER2), 21.6% (HCER3), 8.4% (HCER4), 13.4% (HCER5 + HCER6 + HCER8), 15.3% (HCER7). To check the purity of CER1-lin, CER1-ol, and CER1-ste gas chromatography analysis was performed. CER1-ol and CER1-ste were indeed 100% C18:1 and C18:0, respectively. CER1-lin consisted of several fractions, of which 78% was C18:2 and 14% C18:1.

Lipid organization The lipid organization was studied at pH 5 and pH 7.4. As no differences in phase behavior were observed, we only present the studies carried out at pH 5.

Lateral packing: FFA facilitate the formation of orthorhombic sublattice; presence of unsaturated C18 acyl chain is required for the formation of the liquid phase The results obtained on lateral packing and lamellar phase in lipid mixtures studied are summarized in **Table I.** Due to the small cross-section of the wide angle X-ray diffraction beam, it should be noted that the intensities of the CHOL reflection, presented in **Table II**, approach the average values of the entire sample much better than values given in **Table I**.

CHOL:HCER mixtures In **Fig 3(*A*)** the diffraction pattern of an equimolar CHOL:HCER mixture is depicted. The pattern is characterized by a large number of strong and weak peaks. A strong peak at a spacing of 0.407 nm indicates the presence of a hexagonal sublattice. In addition, a series of sharp peaks mainly ranging between $Q = 10\ nm^{-1}$ and $Q = 15\ nm^{-1}$ can be attributed to crystalline CHOL and obscures the presence of the broad 0.46 nm reflection. The latter is attributed to the liquid subphase and has been noticed also in a previous study (Bouwstra *et al*, 2001). Addition of FFA induces the formation of orthorhombic lateral packing.

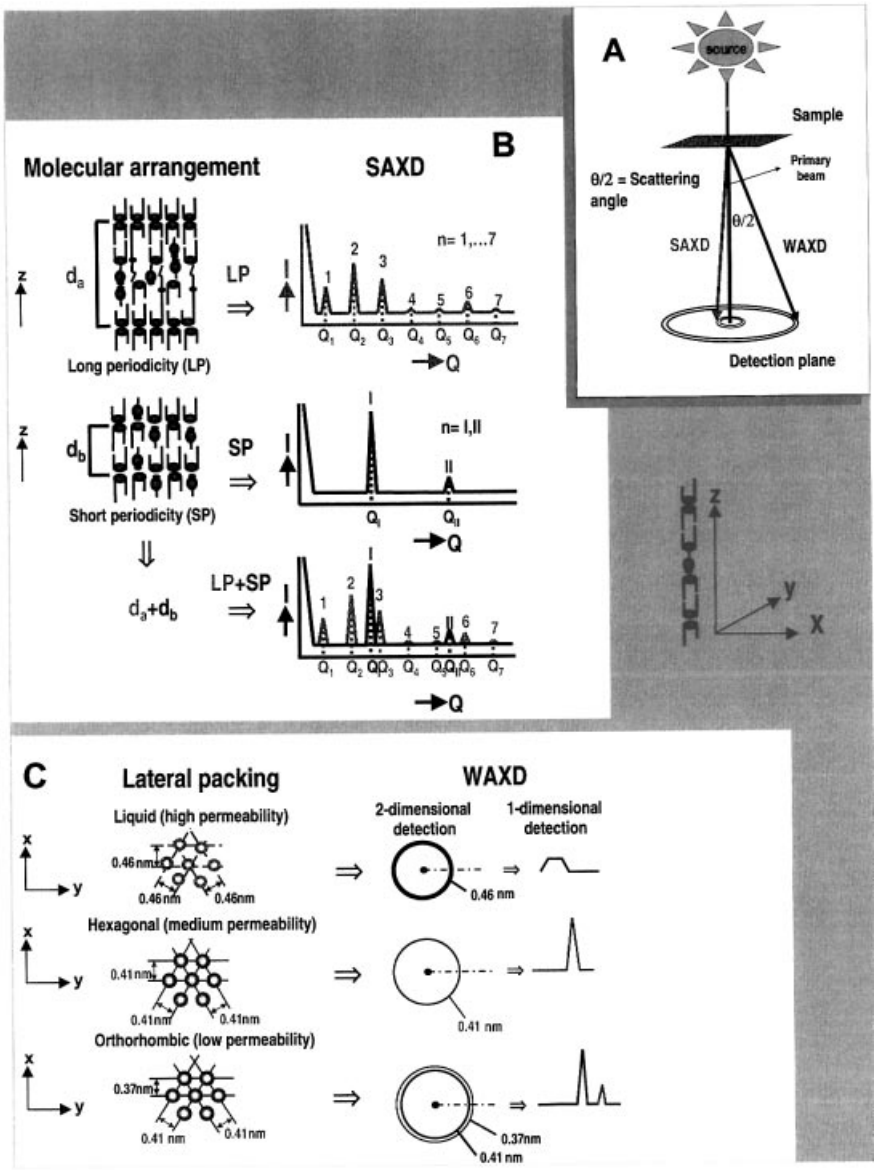

Figure 2. A schematic presentation of the X-ray diffraction technique. (*A*) A source produces X-rays that are partly scattered by the sample. The scattered intensity is measured as a function of the scattering angle $\theta/2$. When the scattered intensity is measured at low angle, the technique provides information about the larger structural units in the sample. In that case the technique is referred to as small angle X-ray diffraction. When the scattered intensity is measured at higher scattering angle, the technique provides information about the smaller structural units such as the lateral packing of the lipids in the lamellae. Often the scattered intensity (I) is plotted as a function of Q, the scattering vector. The scattering vector is related to $\theta/2$ as $Q = 4\pi \sin(\theta)/\lambda$. (*B*) Small angle X-ray diffraction. The intensity of the scattered X-rays is plotted as a function of Q. The diffraction pattern of a lamellar phase consists of a series of peaks, referred to as the first order located at Q_1, second order located at Q_2, third order located at Q_3, etc. As the distance between the sequential peaks is equal, the peak positions are related as $Q_3 = 3Q_1$, $Q_2 = 2Q_1$, etc. From the positions of these peaks the periodicity d_A (in the three-dimensional structure in the z direction) of the lamellar phase can directly be calculated by $d_a = 2\pi/Q_1 = 4\pi/Q_2 = 6\pi/Q_3$, etc. When the repeat distance of the lamellar phase is larger, the distance between the sequential peaks is smaller [compare d_A (LP) with d_B (SP)]. If two lamellar phases (LP + SP) are present in the sample the diffraction peaks of the two phases are additive. This often results in the formation of a broader peak with a shoulder (see, for example, **Fig 4**). Wide angle X-ray diffraction: a schematic presentation of the positions of the alkyl chains in liquid, hexagonal, and orthorhombic phases parallel to the basal plane (i.e., in the x–y direction perpendicular to the z direction) of the lamellae and their corresponding diffraction patterns. In a liquid phase (high permeability) the distances between the hydrocarbon chains is not very well defined resulting in a broad reflection at approximately 0.46 nm. In hexagonal packing (medium permeability) the hydrocarbon chains of the lipids are equally distributed in the structure at interchain distances of 0.48 nm (spacing 0.41 nm). This results in a strong reflection at approximately 0.41 nm spacing. The orthorhombic phase (low permeability) is a very dense structure in which the hydrocarbon chains are not equally distributed in the lattice. This results in a diffraction pattern with two reflections at 0.41 and at 0.37 nm, respectively.

CHOL:HCER(1-ste, 2–8) mixtures The 0.406 nm peak in the diffraction pattern of the equimolar CHOL:HCER(1-ste, 2–8) indicates the formation of hexagonal lateral packing (**Fig 3*B***). A series of sharp peaks are attributed to CHOL that phase-separates in crystalline domains. Addition of FFA reduces the amount of phase-separated crystalline CHOL and leads to a transformation of a hexagonal lateral packing into an orthorhombic packing (**Fig 3*B***). Striking is the absence of a broad 0.46 nm peak. It is obvious that no fluid phase has been formed.

CHOL:HCER(1-ol, 2–8) mixtures In equimolar ratio CHOL:HCER(1-ol, 2–8) a hexagonal lateral sublattice is formed (peak at

Table I. The lateral packing of the lipid mixtures[a]

Composition (molar ratio)	Hex	Ortho	Liquid	CHOL
Mixtures with HCER				
CHOL:HCER = 1:1	+	–	±	+
CHOL:HCER:FFA = 1:1:1	–	+	+	±
Mixtures with HCER(2–8) + synthetic HCER 1 (10% wt/wt)				
CHOL:HCER(1-ste, 2–8) = 1:1	+	–	–	+
CHOL:HCER(1-ste, 2–8):FFA = 1:1:1	–	+	–	–
CHOL:HCER(1-ol, 2–8) = 0.2:1	+	–	–	–
CHOL:HCER(1-ol, 2–8) = 0.6:1	+	–	±	±
CHOL:HCER(1-ol, 2–8) = 1:1	+	–	±	±
CHOL:HCER(1-ol, 2–8):FFA = 1:1:1	–	+	+	–
CHOL:HCER(1-ol, 2–8):FFA = 1:1:1 (pH = 7.4)	–	+	+	–
CHOL:HCER(1-ol, 2–8):FFA:CS = 1:1:1:0.15	–	+	+	–
CHOL:HCER(1-lin, 2–8):FFA:CS = 1:1:1:0.15	–	+	+	±
CHOL:HCER(1-lin, 2–8) = 0.2:1	+	–	–	+
CHOL:HCER(1-lin, 2–8) = 0.4:1	+	–	–	–
CHOL:HCER(1-lin, 2–8) = 1:1	+	–	±*	+
CHOL:HCER(1-lin, 2–8):FFA = 1:1:1	–	+	±*	+
CHOL:HCER(1-lin, 2–8):FFA = 1:1:1 (pH = 7.4)	–	+	±*	+

[a]Because of the small cross-section of the wide angle X-ray diffraction beam, the intensities of the CHOL reflection presented in Table II approach much better the average values of the entire sample than the values given in this table. Hex, hexagonal lateral packing; Ortho, orthorhombic lateral packing; CS, cholesterol sulfate; +, strongly present; ±, weakly present; –, not present; *, liquid phase difficult to identify due to the presence of CHOL reflections.

Table II. The lamellar phases and crystalline CHOL in the lipid mixtures[a]

Composition (molar ratio)	LPP	SPP	CHOL
Mixtures with HCER			
CHOL:HCER = 1:1	12.8 (1, 2, 3, 6, 7)	5.4 (1, 2)?	+
CHOL:HCER:FFA = 1:1:1	13 (2, 3, 6)	5.5 (1, 2, 3, 4)	
Mixtures with HCER (2–8) + synthetic HCER 1			
CHOL:HCER(ste 1, 2–8) = 1:1	–	5.6 (1)	+
CHOL:HCER(ste 1, 2–8):FFA = 1:1:1	–	6.3 (1)	+
CHOL:HCER(ol 1, 2–8) = 0.1:1	12.8 (1, 2, 3, 4, 6, 7)	–	–
CHOL:HCER(ol 1, 2–8) = 0.6:1	12.8 (1, 2, 3, 6, 7)	5.2 (1, 2)	+
CHOL:HCER(ol 1, 2–8) = 1:1	12.8 (1, 2, 3, 4, 6)	5.2 (1, 2)	+
CHOL:HCER(ol 1, 2–8):FFA = 1:1:1	12.8 (2, 3, 4, 6)	5.6 (1, 2, 3)	+
CHOL:HCER(ol 1, 2–8):FFA = 1:1:1 (pH 7.4)	12.8 (2, 3, 4, 6)	5.6 (1, 2, 3)	+
CHOL:HCER(ol 1, 2–8):FFA:CS = 1:1:1:0.15	12.7 (1, 3, 6)	5.7 (1, 2, 3, 4)	±
CHOL:HCER(lin 1, 2–8) = 0.2:1	13.0 (1, 2, 3, 4, 6)	5.5 (1, 2, 3, 4)	–
CHOL:HCER(lin 1, 2–8) = 1:1	13.0 (1, 2, 3)	5.5 (1)	+
CHOL:HCER(lin 1, 2–8):FFA:CS = 1:1:1	13.0 (1, 2, 3, 4, 6)	5.5 (1, 2, 3, 4)	±

[a]A question mark indicates that the presence of this phase is uncertain. CS, cholesterol sulfate; +, strongly present; ±, weakly present; –, not present; 12.8 (1, 2, 3, 4, 6, 7) means periodicity is 12.8 nm, and interpretation is based on the presence of the first, second, third, sixth, and seventh order reflections.

0.409 nm, see **Fig 3*C***). At this molar ratio crystalline CHOL phase separates. Decreasing the CHOL level to a 0.6:1 molar ratio in the CHOL:HCER(1-ol, 2–8) mixture does not change the lateral packing (not shown). The slope of the 0.409 nm peak is less steep on the left-hand side than on the right-hand side, however, indicating the presence of a fluid phase. A further reduction to 0.2:1 CHOL:HCER(1-ol, 2–8) molar ratio results in disappearance of the CHOL reflections in the diffraction pattern. The lateral packing is still hexagonal as can be deduced from the presence of the 0.408 nm peak (not shown).

Addition of FFA to achieve an equimolar CHOL:CER(1-ol, 2–8):FFA mixture induces a transformation from hexagonal to orthorhombic lateral packing (**Fig 3*C***). This transition can be deduced from the appearance of an additional 0.365 nm peak in the diffraction pattern. Furthermore, a liquid phase (broad 0.46 nm) coexists with the orthorhombic lateral packing. The peaks attributed to crystalline CHOL almost disappear, indicating that FFA strongly increase the solubility of CHOL in the lamellar phases. The higher order reflections of the lamellar phases are also indicated in **Fig 4(*D*)**.

CHOL:HCER(1-lin, 2–8) mixtures Equimolar 1:1 CHOL:HCER(1-lin, 2–8) mixtures revealed the formation of a hexagonal lateral sublattice, as can be concluded from the presence of the 0.409 nm peak in the diffraction pattern (see **Fig 3*D***). Reduction to an 0.2:1 CHOL:HCER(1-lin, 2–8) molar ratio does not change the lateral packing (not shown).

Addition of FFA results in a transition from hexagonal to orthorhombic lateral packing (**Fig 3*D***). Although a fluid phase might be present in these equimolar mixtures in the presence and absence of FFA, this broad peak is obscured by the presence of a large number of CHOL reflections.

Small angle X-ray diffraction: both the degree of saturation of the C18 acyl chain of CER1 and the presence of FFA affect the formation of the LPP and the solubility of CHOL A summary of the data is provided in **Table II**. A more detailed description is given below.

CHOL:HCER mixtures The diffraction curve of the equimolar CHOL:HCER mixture is given in **Fig 4**. Five (first, second, third, sixth, and seventh order) diffraction peaks are attributed to a

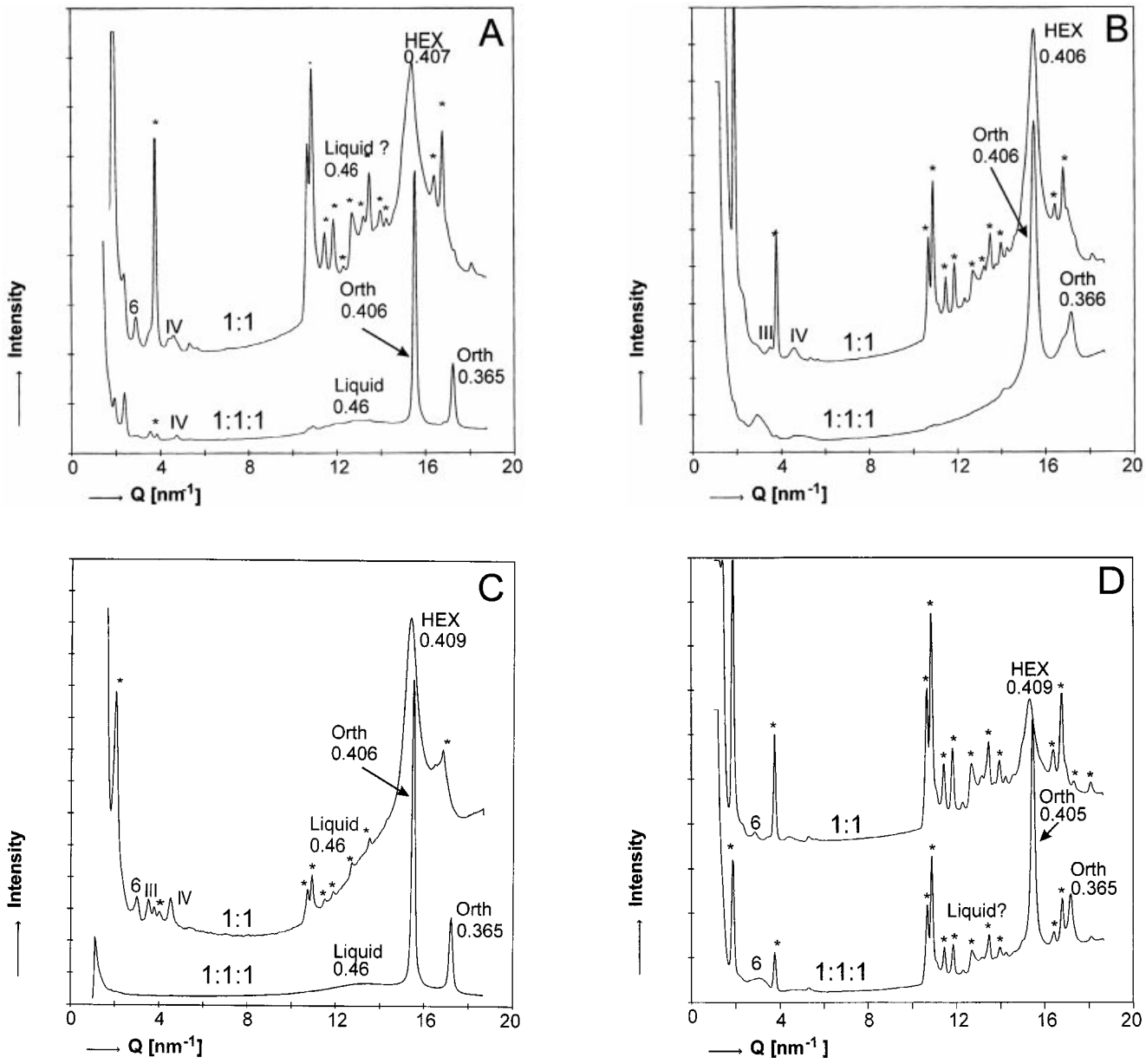

Figure 3. Lateral packing of mixtures prepared with HCER, HEX, Orth, and Liq denote reflections attributed to hexagonal, orthorhombic, and liquid lateral packing, respectively. An asterisk indicates a reflection attributed to crystalline CHOL. The arabic numbers indicate the diffraction orders of the LPP. The roman numbers indicate the diffraction orders of the SPP. The third and fourth order reflections of the 5.4 nm phase, however, are at approximately the same position as the seventh and ninth order reflections of the 12.8 nm lamellar phase. These reflections cannot therefore be distinguished. (*A*) The lateral packing of CHOL:HCER(1–8) and CHOL:HCER(1–8):FFA mixtures. (*B*) The lateral packing of CHOL:HCER(1-ste, 2–8) and CHOL:HCER(1-ste, 2–8):FFA mixtures. (*C*) The lateral packing of CHOL:HCER(1-ol, 2–8) and CHOL:HCER(1-ol, 2–8):FFA mixtures. (*D*) The lateral packing of CHOL:HCER(1-lin, 2–8) and CHOL:HCER(1-lin, 2–8):FFA mixtures.

lamellar phase with a repeat distance of 12.8 nm (LPP). Whether an SPP is also present in the mixture is not clear from the diffraction pattern, as the presence of the first order diffraction at approximately 5.4 nm spacing is not obvious. Based on the asymmetry of the 4.5 nm peak, the third order peak (of the LPP), and an additional peak located at a spacing of 2.7 nm (second order), however, it was concluded that a small fraction of lipids forms the SPP. Additionally, two peaks are attributed to crystalline phase-separated CHOL. Addition of FFA promoted the formation of the SPP (periodicity 5.5 nm) as can be deduced from the presence of the first, second, third, and fourth order peaks of this lamellar phase. The 13 nm lamellar phase is also present in the mixture. Namely, at both sides of the 5.5 nm peak (first order of SPP) a shoulder is present indicating the second and third order peaks of the LPP. In addition, the sixth order diffraction peak of the 13 nm lamellar phase is present. Furthermore, the third and fourth order peaks of the SPP might also be attributed to the 13 nm lamellar phase, being then the seventh and ninth order diffraction peaks, respectively, as these are located at approximately the same position. The peaks attributed to CHOL are still present but reduced in peak intensity.

CHOL:HCER(1-ste, 2–8) mixture In **Fig 5** the diffraction peaks of the equimolar CHOL:HCER(1-ste, 2–8) mixture are plotted. A strong broad peak (first order) and a weak peak (second order) are both attributed to the SPP (periodicity 5.6 nm). No LPP has been

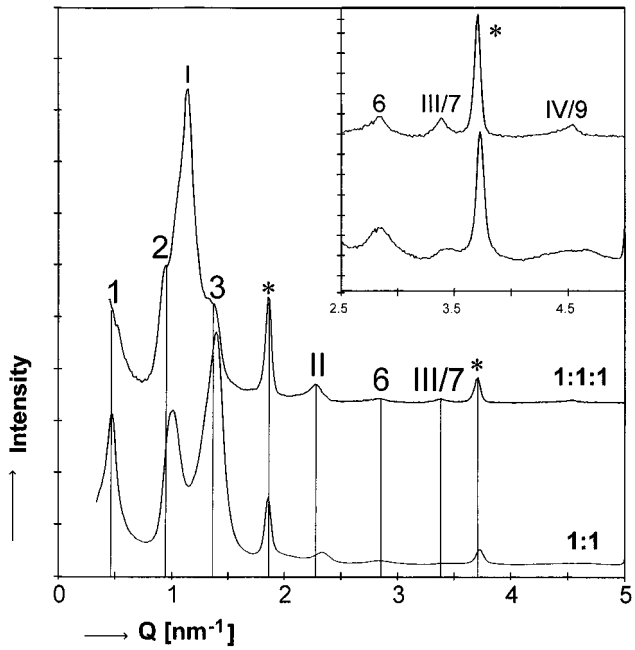

Figure 4. The diffraction profiles of the equimolar CHOL:HCER(1–8) and CHOL:HCER(1–8):FFA mixtures at pH 5. The peaks indicated by the arabic number in the figure are atributed to the LPP; the peaks indicated by a roman number are attributed to the SPP. An asterisk indicates the peaks at 3.33 nm (Q = 1.88 nm^{-1}) and 1.69 nm (Q = 3.71 nm^{-1}) attributed to crystalline CHOL. Equimolar (1:1) CHOL:HCER(1–8) mixtures: the peaks located at a spacing of 13 nm (Q = 0.48 nm^{-1}), 6.2 nm (Q = 1.01 nm^{-1}), 4.5 nm (Q = 1.39 nm^{-1}), 2.2 nm (Q = 2.85 nm^{-1}), and 1.89 nm (Q = 3.32 nm^{-1}) are attributed to a long periodicity lamellar phase (first, second, third, sixth, and seventh order) with a repeat distance of 12.8 nm. The peak located at a spacing of 2.7 nm (Q = 2.32 nm^{-1}) is interpreted as being second order (indicated by II) of the 5.4 nm phase. Equimolar (1:1:1) CHOL:HCER(1–8):FFA mixtures: a lamellar phase with a periodicity of 5.5 nm is clearly present, as can be deduced from the peaks located at 5.5 nm (Q = 1.14 nm^{-1}, first order), 2.77 nm (Q = 2.26 nm^{-1}, second order), 1.85 nm (Q = 3.40 nm^{-1}, third order), and 1.35 nm (Q = 4.65 nm^{-1}, fourth order) spacing. The shoulders with spacings of 6.2 nm (Q = 1.01 nm^{-1}, second order) and 4.5 nm (Q = 1.39 nm^{-1}, third order) and the peak at 2.23 nm (Q = 2.81 nm^{-1}, sixth order) are attributed to the lamellar phase with a periodicity of 13 nm.

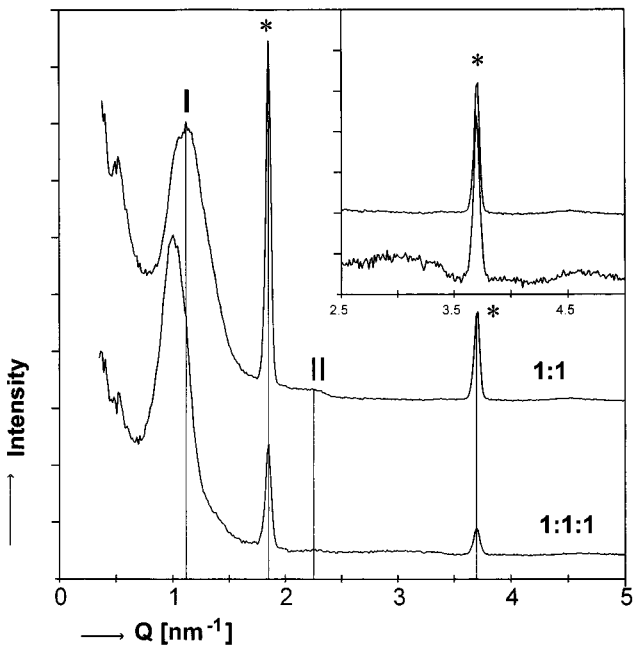

Figure 5. The diffraction profile of the equimolar CHOL:HCER(1-ste, 2–8) and CHOL:HCER(1-ste, 2–8):FFA mixtures. The roman numbers indicate the diffraction orders of the SPP. An asterisk indicates the reflections at 3.33 nm (Q = 1.88 nm^{-1}) and 1.69 nm (Q = 3.71 nm^{-1}) attributed to crystalline CHOL. Equimolar CHOL:HCER(1-ste, 2–8) mixtures: peaks located at 5.6 nm (Q = 1.12 nm^{-1}, first order) spacing and at 2.8 nm (Q = 2.24 nm^{-1}, second order) spacing are attributed to a phase with a periodicity of 5.4 nm. Equimolar CHOL:HCER(1-ste, 2–8):FFA mixtures: a peak located at 6.2 nm (Q = 0.98 nm^{-1}) is attributed to the SPP.

formed in this mixture. Addition of FFA increases the periodicity of the lamellar phase to 6.3 nm, and reduces the amount of CHOL that is present in separate crystalline domains.

CHOL:HCER(1-ol, 2–8) mixtures The diffraction curve of the equimolar CHOL:HCER(1-ol, 2–8) mixture is plotted in **Fig 6(*A*).** Four peaks (first, second, third, and sixth order) are attributed to the LPP with a repeat distance of 12.8 nm. An SPP is also present in the mixture as can be deduced from its broad first order diffraction peak. Additionally, two peaks are attributed to phase-separated crystalline CHOL.

Reduction in CHOL level to an 0.6:1 CHOL:HCER(1-ol, 2–8) molar ratio does not change the positions of the peaks attributed to the lamellar phases (**Fig 6*A***). A further reduction to a molar ratio of 0.2 results in a decrease in the intensity of the first order peak of the SPP. In this curve higher order reflections of the LPP can also be detected. In addition, the peaks attributed to crystalline CHOL disappear.

The phase behavior of the equimolar CHOL:HCER(1-ol, 2–8):FFA mixture is shown in **Fig 6(*B*)**. The presence of the LPP with a periodicity of 12.6 nm is indicated by the second, third, sixth, and seventh order diffraction peaks. Furthermore, the first, second, and third order peaks of the 5.6 nm lamellar phase (SPP) are also detected. The latter can also be attributed to the 12.6 nm phase (seventh order). Crystalline CHOL is also present in the mixture. Addition of cholesterol sulfate increases the width of the peaks (**Fig 6*B***). The presence of the first, third, and sixth order peaks of the 12.7 nm lamellar phase clearly indicates that the LPP is formed. As the second and third order of the 5.6 nm phase are also clearly present, most probably the SPP is formed as well. It seems that due to the increase in peak width, the second order peak of the LPP (spacing 6.3 nm) and the first order of the SPP (spacing 5.6 nm) cannot be distinguished and turn into one broad peak.

CHOL:HCER(1-lin, 2–8) mixtures The diffraction curves of the CHOL:HCER(1-lin, 2–8) mixtures are plotted in **Fig 7(*A*)**. In the curve of the 0.2:1 mixture four diffraction peaks (first, second, third, and fourth) attributed to a 13 nm lamellar phase are present. In addition, the first, second, and third order peaks of the SPP with a repeat distance of 5.5 nm phase are detected. Increasing the CHOL content to achieve an equimolar mixture does not change the phase behavior dramatically except for an increase in the amount of phase-separated CHOL. After addition of FFA the presence of the LPP is more prominent (**Fig 7*B***), as the first, second, and third order peaks attributed to the LPP are strong. The intensity of the diffraction peaks attributed to the SPP is slightly reduced.

Peak intensity calculations: the LPP:SPP peak intensity ratio can be correlated with the liquid:crystalline peak intensity ratios Peak intensity ratios were calculated that were indicative for the relative presence of LPP/SPP and liquid/crystalline phases. Due to the overlap of the various peaks, the interference with the CHOL peaks, and the nature of the peak attributed to the liquid phase, however, we decided not to provide peak ratios of individual mixtures. For the peak intensity ratios of the liquid:crystalline phases we clearly found four categories corresponding to a liquid:crystalline peak ratio of approximately

0, 0.1, 0.3, and 0.6. Based on the calculations the following ranking of the LPP:SPP peak ratios has been made: zero, for an LPP:SPP peak ratio of 0; low, for ratios between 0 and 1; medium, for ratios between 1 and 2; high, for LPP:SPP ratios higher than 2. The LPP:SPP peak intensity ratio is plotted against the liquid:crystalline peak ratio for the various mixtures in **Fig 8.**

DISCUSSION

The main objective of this study was to investigate the role of HCER1 on lipid phase behavior and on lateral packing in lipid mixtures based on CHOL, HCER, and FFA with a special focus on the moiety of fatty acid ester linked to the ω-hydroxy acid. In mixtures prepared with CHOL:HCER a lamellar phase with a periodicity of 12.8 nm (referred to as the LPP) can clearly be detected. In a previous study it has been shown that in the absence of HCER1 the situation is different. In an equimolar CHOL:HCER(2–8) mixture only a small fraction of lipids forms the LPP: a lamellar phase with a periodicity of 5.3 nm (referred to as the SPP) predominates (Bouwstra *et al*, 2001). From this observation we conclude that, similarly to mixtures prepared with pigCER (Bouwstra *et al*, 1998a), HCER1 plays an important role in the formation of the LPP. These observations also indicate that HCER4, with a similar structure to HCER1, seems to play a minor role for the formation of the LPP. When extrapolating these findings to the *in vivo* situation, a reduction of HCER1 content, as found in atopic dermatitis patients or dry skin, may lead to alteration of the organization of lamellar phases. Recently, indeed, a relationship between a reduced HCER1 level and a reduction of the LPP has been reported for the *in vivo* situation (Schreiner *et al*, 2000).

As judged from this study even more detailed conclusions can be drawn on the role of CER1 in the formation of the LPP. Namely, the formation of the LPP was affected by the acyl chain moiety of HCER1. Surprisingly, the fraction of lipids forming the LPP was reduced to a greater extent in CHOL:HCER mixtures in which the natural HCER1 was substituted by synthetic CER1-lin than in mixtures containing HCER1-ol. Not only the lamellar phase behavior but also the lateral packing was affected by the acyl chain structure of HCER1 (schematically summarized in **Fig 9**). Thus the presence of a liquid phase was observed when the CHOL: HCER mixture contained HCER1 with an unsaturated C18 acyl chain as in natural HCER1, synthetic CER1-ol, or synthetic CER1-lin, but not with CER containing the saturated C18 fatty acid, as in synthetic CER1-ste. It seems that the presence of an unsaturated C18 acyl chain linked to the ω-hydroxyl acyl chain of HCER1 is a prerequisite for the formation of the liquid phase. Furthermore, although not quantified, our data strongly suggest that the liquid phase is more prominently present in mixtures containing synthetic CER1-ol than synthetic CER1-lin. This might be related to a larger volume of the oleate moiety (void volume 7.18 nm^2) in comparison to the linoleate moiety (6.23 nm^2) (C. Harding, personal communication).

In **Fig 8** the estimated LPP:SPP peak ratios are plotted against the liquid:crystalline peak ratio. This figure indicates that for the formation of the LPP a certain (optimal) fraction of lipids has to be present in a liquid sublattice. When the fraction of lipids forming the liquid sublattice is small, the LPP dominates the SPP. On the other hand, when the liquid:crystalline ratio is too low (as in

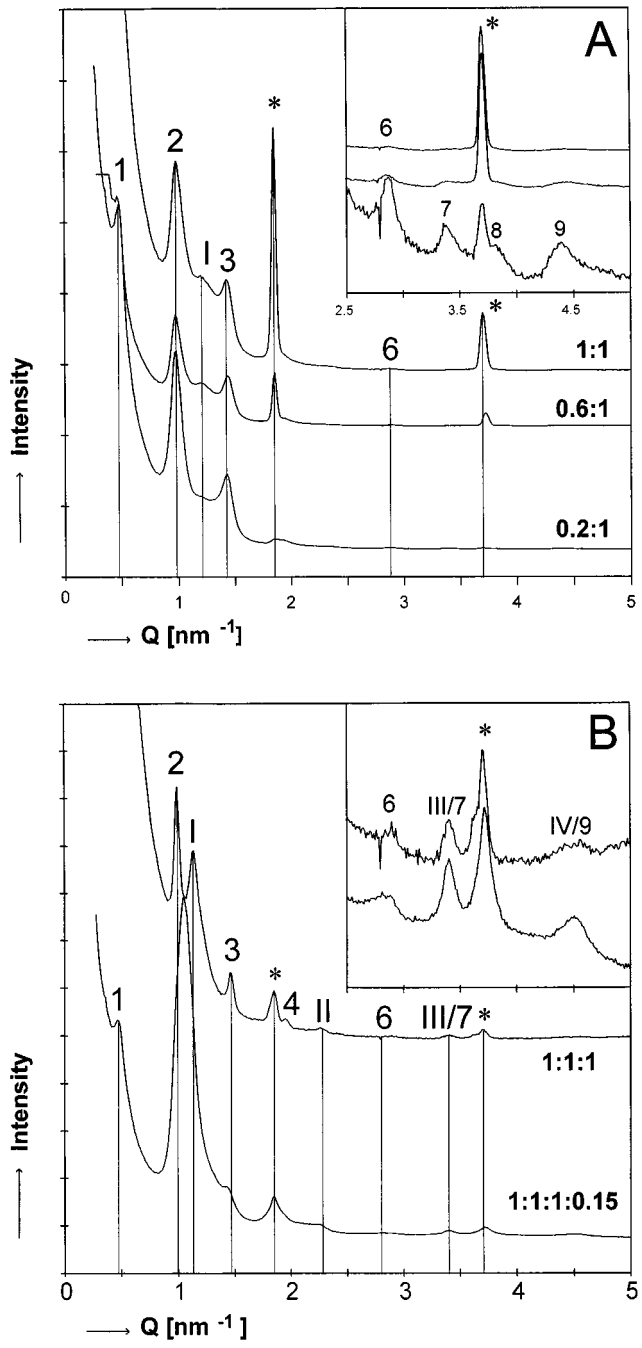

Figure 6. The diffraction profile of the CHOL:CER(1-ol, 2–8) and CHOL:CER(1-ol, 2–8): FFA mixtures. (*A*) The effect of CHOL:HCER(1-ol, 2–8) molar ratio on the phase behavior. The arabic numbers indicate the diffraction orders of the LPP (repeat distance 12.8 nm). The roman numbers indicate the diffraction orders of the SPP (repeat distance 5.4 nm). The asterisk indicates a reflection attributed to crystalline CHOL. The CHOL:HCER molar ratios are indicated in the figure. No changes in peak positions are observed when the CHOL:HCER molar ratio is changed. Four peaks located at a spacing of 12.8 nm ($Q = 0.49\ nm^{-1}$), 6.3 nm ($Q = 1.00\ nm^{-1}$), 4.4 nm ($Q = 1.43\ nm^{-1}$), and 2.2 nm ($Q = 2.86\ nm^{-1}$) are attributed to a lamellar phase (first, second, third, and sixth order) with a repeat distance of approximately 12.8 nm. A broad peak at 5.2 nm ($Q = 1.20\ nm^{-1}$) is attributed to the SPP with a repeat distance of approximately 5.2 nm. At the 0.2:1 CHOL:HCER molar ratio the seventh, eighth, and ninth order reflections attributed to the 12.8 nm phase are also detected. (*B*) The phase behavior of equimolar CHOL:HCER:FFA mixtures (1:1:1) at pH 5. Diffraction peaks located at 6.3 nm ($Q = 1.00\ nm^{-1}$), 4.3 nm ($Q = 1.46\ nm^{-1}$), 2.2 nm ($Q = 2.86\ nm^{-1}$) 1.8 nm ($Q = 2.24\ nm^{-1}$), and 1.39 nm ($4.4\ nm^{-1}$) spacing are second, third, sixth, seventh, and ninth order diffraction peaks of a 12.6 nm lamellar phase. The diffraction peaks at 5.6 nm ($Q = 1.12\ nm^{-1}$, first order), 2.8 nm ($Q = 2.24\ nm^{-1}$, second order), and 1.8 nm ($Q = 2.24\ nm^{-1}$, third order) spacing are attributed to a 5.6 nm lamellar phase. The 1.8 nm peak can also be attributed to the 12.6 nm phase (seventh order). After addition of cholesterol sulfate the second order of the 12.5 nm phase and the first order of the 5.6 nm phase turn into one peak.

mixtures containing CER1-ste) or too high [as in HCER and HCER(1-ol, 2–8) mixtures containing FFA] the SPP starts to dominate the LPP. These observations further indicate the interplay between the individual SC major lipid components and that changes in their composition and/or relative content will determine the final SC lipid organization.

As already suggested in a previous study (Bouwstra *et al*, 2001) the liquid phase is more prominently present in HCER mixtures compared to pigCER mixtures. This can also be explained by the increased fraction of linoleic/oleic acid linked to the ω-hydroxy acid chain. In HCER mixtures this amounts to about 17.8% wt/wt (HCER1 + HCER4), whereas in the pigCER mixture used in our previous studies (Bouwstra *et al*, 1996) this fraction was 8% wt/wt (pigCER1).

The results obtained in this paper can broaden our knowledge on the mechanisms leading to the perturbation of the SC organization and barrier function in diseased skin. (i) In skin diseases in which the HCER1-ol:HCER1-lin ratio is increased above the level found in normal skin, such as in essential fatty acid deficient skin and in skin during the winter season, the formation of a fluid phase will be promoted. It should be noted, however, that when the fraction of lipids forming the fluid phase is too high a perturbation of the barrier function may occur. Although it has been demonstrated that lamellar phases are still formed in essential fatty acid deficient skin

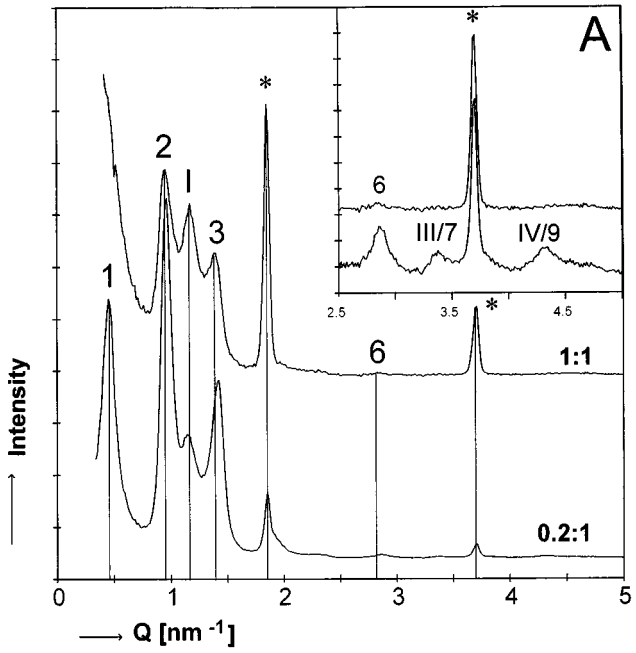

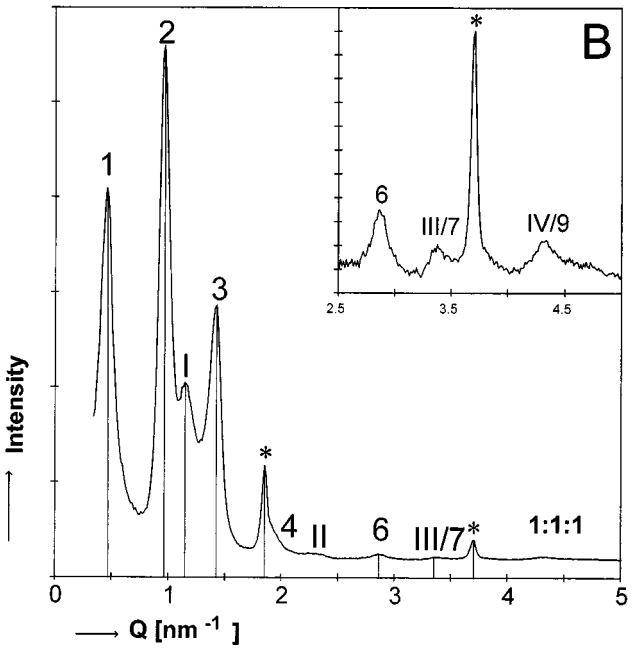

Figure 7. The diffraction profile of the CHOL:HCER(1-lin, 2–8) and CHOL:HCER(1-lin, 2–8): FFA mixtures. (*A*) The effect of CHOL:HCER(1-lin, 2–8) molar ratio on the phase behavior. The CHOL:HCER molar ratios are indicated in the figure. The arabic numbers refer to the diffraction orders of the LPP (repeat distance 12.8 nm). The roman numbers indicate the diffraction orders of the SPP (repeat distance 5.4 nm). The asterisk indicates the reflections at 3.33 nm (Q = 1.88 nm^{-1}) and 1.69 nm (Q = 3.71 nm^{-1}) attributed to crystalline CHOL. In the curve of the 0.2:1 mixture the diffraction peaks at 13 nm (Q = 0.48 nm^{-1}), 6.5 nm (Q = 0.97 nm^{-1}), 4.4 nm (Q = 1.42 nm^{-1}), 3.3 nm (Q = 1.90 nm^{-1}), 2.2 nm (Q = 2.86 nm^{-1}) spacing are attributed to the 13 nm lamellar phase (first, second, third, fourth, sixth, and ninth order). The 5.5 nm (Q = 1.14 nm^{-1}), 2.8 nm (Q = 2.24 nm^{-1}), and 1.86 nm (Q = 3.38 nm^{-1}) peaks are due to the 5.5 nm lamellar phase (first, second, and third order). (*B*) The phase behavior of equimolar CHOL:HCER:FFA mixtures (1:1:1). Strong peaks present at 6.4 nm (Q = 0.98 nm^{-1}, second order) and 4.4 nm (Q = 1.42 nm^{-1}, third order) spacing are attributed to the 13 nm lamellar phase (arabic numbers). The intensities of peaks located at 5.5 nm (Q = 1.14 nm^{-1}, first order), 2.8 nm (Q = 2.24 nm^{-1}, second order), 1.86 nm (Q = 3.38 nm^{-1}, third order), and 1.39 nm (Q = 4.5 nm^{-1}) are attributed to the 5.5 nm phase (roman numbering). The third and fourth order reflection can also be attributed to the 13 nm phase (seventh and ninth order reflection). The asterisk denotes the reflections attributed to CHOL.

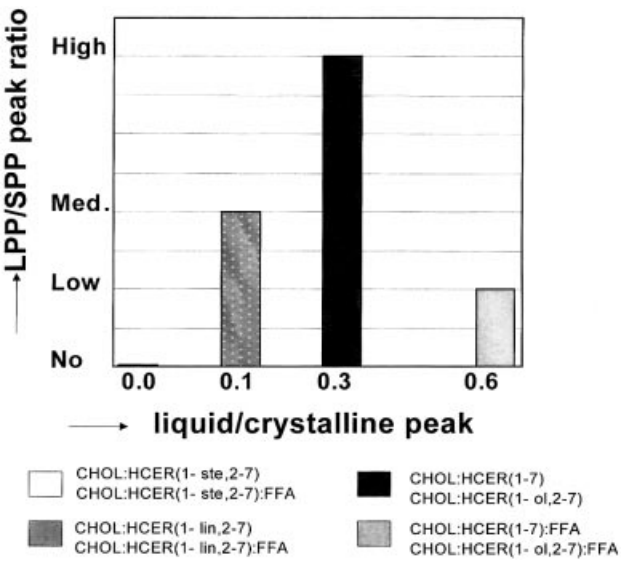

Figure 8. Quantification resulted in liquid:crystalline (liquid: hexagonal in the absence of FFA and liquid:orthorhombic in the presence of FFA) peak ratios of the lipid mixtures. In CHOL:HCER(1-lin, 2–8) mixtures the presence of a liquid phase is less obvious than in HCER(1-ol, 2–8)-containing mixtures, whereas in the HCER and HCER(1-ol, 2–8) mixtures the liquid phase is more prominently present after addition of FFA. In the HCER(1-ste, 2–8)-containing mixtures no liquid phase has been found. The LPP:SPP has been categorized as zero (no LPP), low (LPP:SPP peak ratio between 0.0 and 1), medium (LPP:SPP peak ratio between 1 and 2), and high (LPP:SPP ratio higher than 2). The LPP:SPP peak ratio is according to the equation: second and third order peak intensity of the LPP/(first order peak intensity SPP). The liquid:crystalline ratio is according to peak intensity of the 0.46 nm spacing of the liquid phase divided by either the 0.41 nm peak intensity of the hexagonal phase or the 0.41 and 0.367 nm peak intensities of the orthorhombic phase.

(Melton *et al*, 1987; Hou *et al*, 1991), a further increase in the fraction of lipids forming the fluid phase might (according to **Fig 8**) even disturb the formation of the LPP. This is expected to reduce the skin barrier even further. (ii) In X-linked ichthyosis skin a substantial increase in cholesterol sulfate level has been observed (Elias *et al*, 1984). In a previous study with pigCER it was shown that an increased level of cholesterol sulfate promotes the formation of a fluid phase (Bouwstra *et al*, 1998a; Bouwstra *et al*, 1999). For this reason the elevated levels of cholesterol sulfate in X-linked ichthyosis skin are expected to promote the formation of a fluid phase and possibly also to disturb the formation of the LPP. This will certainly contribute to an impaired skin barrier function in X-linked ichthyosis skin. (iii) In all samples studied so far, the addition of long chain FFA to the CHOL:HCER mixtures results in a hexagonal–orthorhombic transition. This leads to an increase in the lattice density and thereby to the reduction of its permeability as the orthorhombic phase is less permeable than the hexagonal phase. This is in agreement with the findings made in lamellar ichthyosis patients where a reduced level of FFA (Lavrijsen *et al*, 1995) is accompanied by a strong increase in the formation of hexagonal packing (Pilgram *et al*, 2001). This may account at least partly for the impaired barrier in lamellar ichthyosis skin. All the above examples demonstrate an excellent *in vitro–in vivo* correlation between lipid composition, organization, and barrier function and support the usefulness of studies with lipid mixtures based on CERs extracted from human skin for understanding the mechanisms leading to the altered lipid organization in diseased skin.

Based on the results obtained earlier with pigCER (Bouwstra *et al*, 1998a) and the results obtained in this study we propose a model for the molecular arrangement of CHOL and HCER in the LPP (**Fig 10**). This model is similar to that proposed for the mixture of CHOL and pigCER (Bouwstra *et al*, 1998a). In this model, linoleic acid linked to the ω-hydroxy C30–C32 acid of HCER1 and HCER4 together with CHOL is located in the central narrow layer of the 12.8 nm lamellar phase. As the unsaturated acyl chains of HCER1 and HCER4 are important for formation of the liquid phase this phase should be located in the central layer in the LPP. One can speculate that in mixtures containing CER1-ste a reduction in lipid mobility prevents the formation of the fluid central layer (strong van der Waals interactions). On the other hand, a strong increase in the mobility of the central lipid sublattice may induce larger conformational changes of HCER1 and HCER4 (rotation or twisting of single bonds) and might therefore also prevent the formation of the LPP.

If the proposed model is a correct presentation of the real situation, it is of interest to speculate about the permeation routes of small molecules across the SC. It is generally accepted that fluid phases have a much higher permeability (and often solubility) than crystalline phases. Therefore, small molecules would prefer to permeate along the liquid channels or domains located in the central narrow layer of the LPP. This means that permeation in the x–y plane (see **Figs 2**, **10**) parallel to the lamellae would be much faster than permeation perpendicular to the lamellae (z direction, across the head group regions). If indeed the two broad lipid layers adjacent to the central narrow layer are mainly crystalline in nature, the question arises which pathway the permeating agent will take in the direction perpendicular to the lamellar sheets. There are at least three possibilities to circumvent the impermeable crystalline domains, namely (i) permeation between the boundaries of neighboring crystalline domains within one lamellar sheet, (ii) permeation between the boundaries of neighboring lamellar

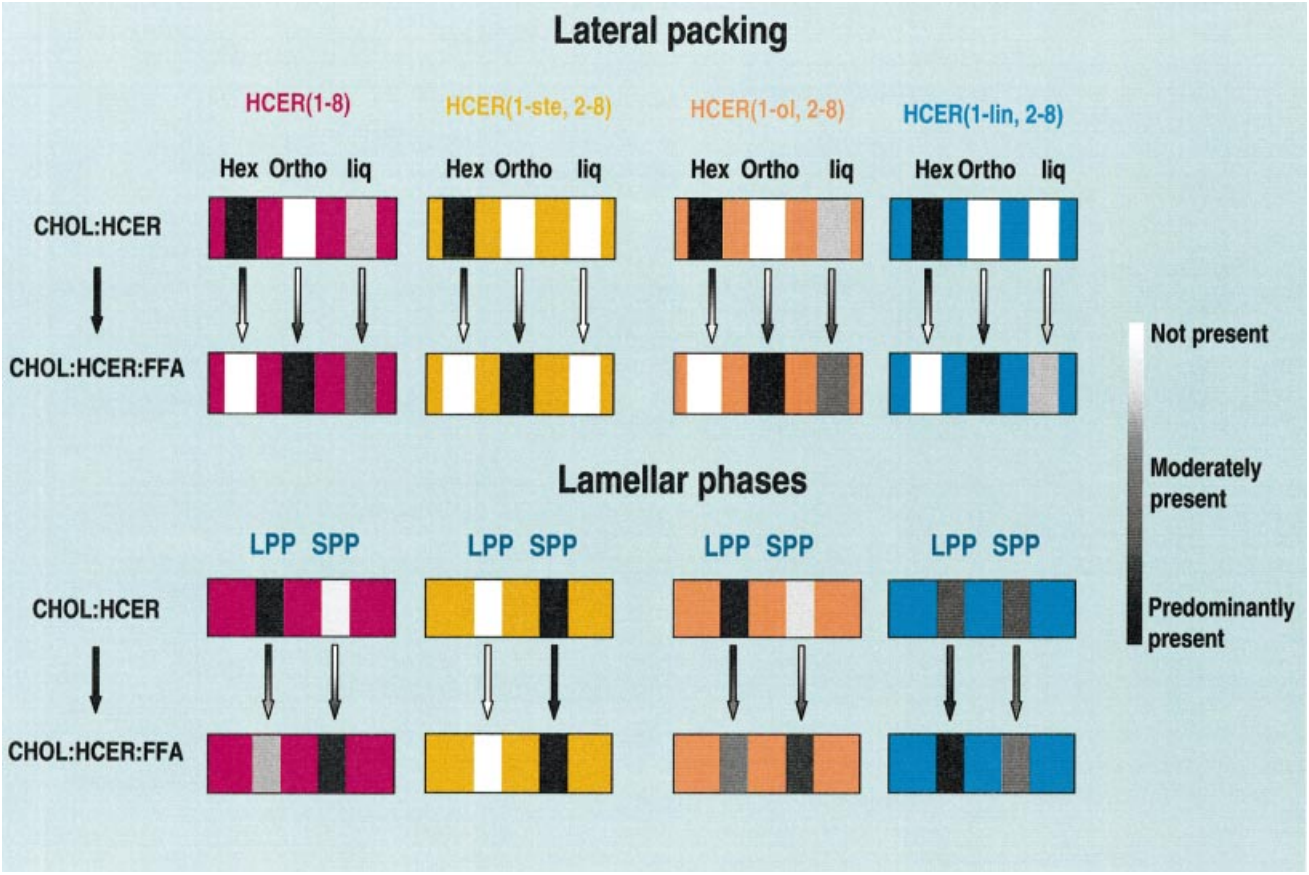

Figure 9. A summary of the lamellar phases and lateral packing in various lipid mixtures. HCER(1–8) mixtures in which HCER1 is replaced by either synthetic CER1-ste (HCER1-ste, 2–8), synthetic CER1-ol (HCER 1-ol, 2–8), or synthetic CER1-lin (HCER1-lin, 2–8).

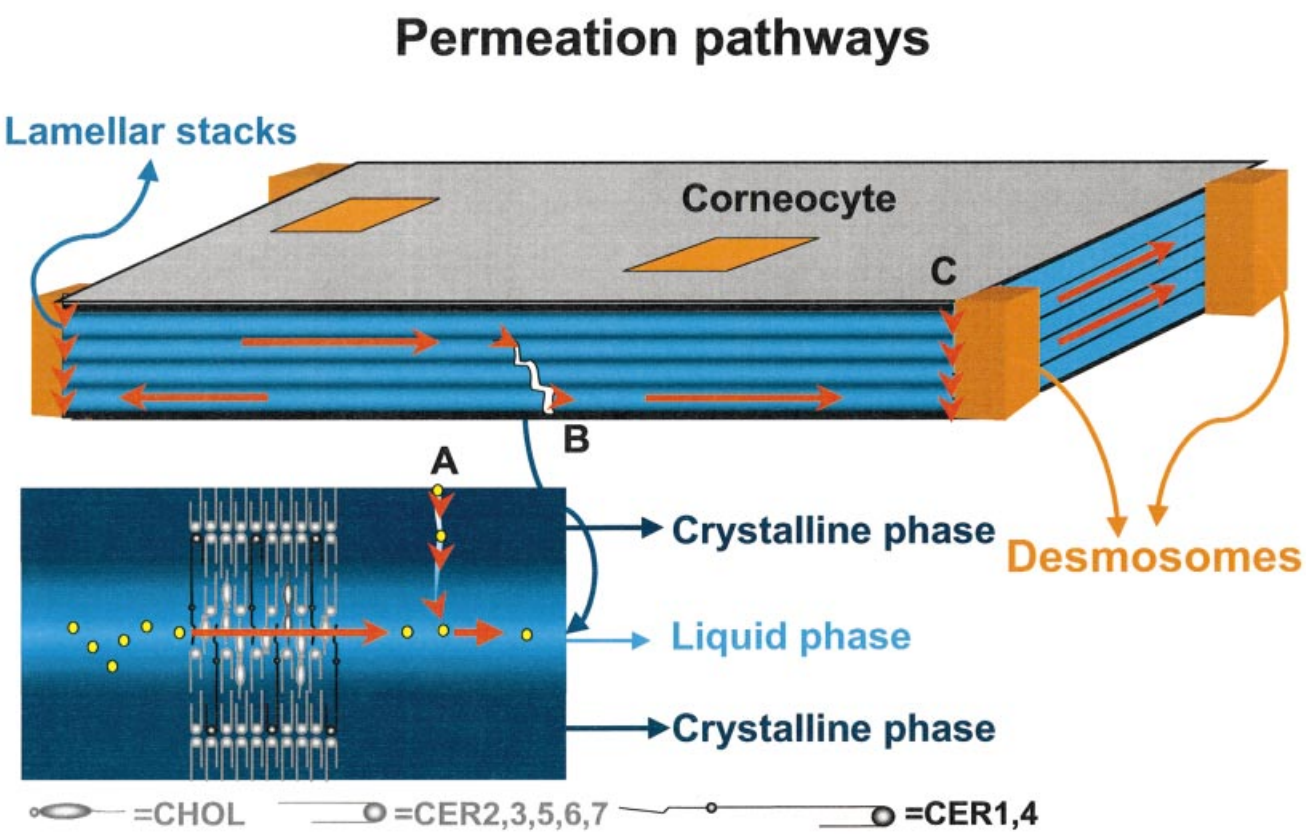

Figure 10. The molecular arrangement of the LPP in HCER:CHOL mixtures. Following this model the repeating unit in the structure consists of three lipid layers. From the model it is obvious that HCER1 and HCER4 are important for the formation of this phase. Furthermore, in the central layer the unsaturated linoleic moiety of HCER1 and HCER4 is located in the central narrow layer of the model. Based on the molecular model we proposed the "sandwich model" (Bouwstra *et al*, 2000). The characteristics are (i) that the liquid sublattice is located in the central lipid layer of this phase. In this layer mainly unsaturated linoleic acid and CHOL are present. (ii) In the sublattice adjacent to the central layer a gradual change in lipid mobility occurs due the presence of less mobile long saturated hydrocarbon chains (see **Fig 1**). This gradual change to crystalline packed lipid layers on both sides of the central layer avoids the formation of new interfaces. (iii) Only a small fraction of lipids forms a fluid phase in the SC. Therefore, one can assume that this central lipid layer is not a continuous fluid phase. (iv) Lamellae are mainly oriented parallel to the surface of the corneocytes. As the liquid phase is the most permeable phase, it is assumed that the penetration pathway of small molecules parallel to the lamellae (x–y direction, see **Fig 2**) is mainly through the liquid channels or domains in the central narrow layer of the LPP (see *large arrows*). This will facilitate communication between the desmosomes. By passing the SC lipid regions in the direction perpendicular to the basal plane (z direction, see **Fig 2**), the crystalline domains can be circumvented (see *arrowheads*) (*A*) by permeation along the boundary between two crystalline domains within a lamellar phase, (*B*) by permeation between the boundaries of two adjacent lamellar sheets, and (*C*) by permeation between the lamellar sheets and desmosomes.

domains, and (iii) permeation between the boundary of a lamellar sheet and the neighboring desmosome. The finding that permeation can be localized in a network of channels, as reported recently by van der Bergh *et al* (1999) after application of fluorescent labels in vesicles, supports our hypothesis. The permeation pathway of water molecules across the SC might be quite exceptional, as water is one of the few molecules that can be taken up by the corneocytes. Therefore, next to permeation along the lipid lamellae, an intracellular penetration pathway in combination with transport along desmosomes might be a possible penetration pathway for this particular molecule. This route in combination with facilitated transport between desmosomes might explain the high water flux across the SC. Future studies are required, however, for verification of the hypotheses.

In conclusion, the results of this study clearly indicate that presence of HCER1 with an unsaturated acyl chain is required for the formation of the LPP as well as for the formation of a liquid phase. The presence of a small fraction of lipids forming a fluid phase might be required for proper elasticity (Forslind, 1994) of the lipid lamella and opens the possibility for molecules to permeate along the lipid lamellae. When the fraction of lipids present in a fluid phase is too high, however, a reduction in barrier function may occur.

We would like to thank Unilever Research United States for financial support of this project.

REFERENCES

Aly R, Shirley C, Cumico B, Maibach HI: Effect of prolonged occlusion on the microbial flora, pH, carbon dioxide and transepidermal water loss on human skin. *J Invest Dermatol* 71:378–381, 1978

van der Bergh BAI, Vroom J, Gerritsen H, Junginger H, Bouwstra JA: Interactions between liquid- and gel-vesicles with human skin *in vitro*: electron microscopy and two photon excitation microscopy. *Biochim Biophys Acta* 1461:155–173, 1999

Bligh EG, Dyer WJ: A rapid method of total lipid extraction and purification. *Can J Biochem Physiol* 37:911–917, 1959

Bouwstra JA, Gooris GS, van der Spek JA, Bras W: Structural investigations of human stratum corneum by small-angle X-ray scattering. *J Invest Dermatol* 97:1005–1012, 1991

Bouwstra JA, Gooris GS, Salomons-de Vries MA, van der Spek JA, Bras W: Structure of human stratum corneum as a function of temperature and hydration: a wide-angle X-ray diffraction study. *Int J Pharm* 84:205–216, 1992

Bouwstra JA, Gooris GS, van der Spek JA, Lavrijsen S, Bras W: The lipid and protein structure of mouse stratum corneum: a wide and small angle diffraction study. *Biochim Biophys Acta* 1212:183–192, 1994

Bouwstra JA, Gooris GS, Bras W, Downing DT: Lipid organization in pig stratum corneum. *J Lipid Res* 36:685–695, 1995

Bouwstra JA, Gooris GS, Cheng K, Weerheim A, Bras W, Ponec M: Phase behavior of isolated skin lipids. *J Lip Res* 37:999–1011, 1996

Bouwstra JA, Gooris GS, Dubbelaar FER, Weerheim AM, IJzerman AP, Ponec M: The role of ceramide 1 in the molecular organisation of SC lipids. *J Lipid Res* 39:186–196, 1998a

Bouwstra JA, Gooris GS, Dubbelaar FER, Weerheim A, Ponec M: pH, cholesterol sulfate and fatty acids affect stratum corneum lipid organisation. *J Invest Dermatol Proc* 3:69–74, 1998b

Bouwstra JA, Gooris GS, Dubbelaar FER, Ponec M: Cholesterol sulfate and calcium affect stratum corneum lipid organization over a wide temperature range. *J Lipid Res* 40:2303–2312, 1999

Bouwstra JA, Gooris GS, Dubbelaar FER, Ponec M: The lipid organisation in the skin barrier. *Acta Derm Venereol* 208:23–30, 2000

Bouwstra JA, Gooris GS, Dubbelaar FER, Ponec M: Phase behaviour of lipid mixtures based on human cermamides, *J Lipid Res* 42:1759–1770, 2001

Chien YL, Wiedmann TS: Human stratum corneum lipids have a disorted orthorhombic packing at the surface of cohesive failure. *J Invest Dermatol* 107:15–19, 1996

Conti A, Rogers J, Verdejo P, Harding CR, Rawlings AV: Seasonal influences on stratum corneum ceramide 1 fatty acids and the influence of topical essential fatty acids. *Int J Cosm Sci* 15:1–12, 1996

Di Nardo A, Wertz P, Giannetti A, Seidenari S: Ceramide and cholesterol composition of the skin in patients with atopic dermatitis. *Acta Derm Venereol (Stockh)* 78:27–30, 1998

Elias PM, Williams ML, Maloney ME, Bonifas JA, Brown BE, Grayson S, Epstein EH: Stratum corneum lipids in disorders of cornification. *J Clin Invest* 74:1414–1421, 1984

Forslind B: A domain mosaic model of the skin barrier. *Acta Derm Venereol* 74:1–6, 1994

Garson J-C, Doucet JC, Lévêque J-L, Tsoucaris G: Oriented structure in human statum corneum revealed by X-ray diffraction. *J Invest Dermatol* 96:43–49, 1991

Gay CL, Guy RH, Golden GM, Mak VM, Francoeur ML: Characterization of low-temperature (i.e. < 65 degrees C) lipid transitions in human stratum corneum. *J Invest Dermatol* 103:233–229, 1994

Hou SY, Mitra AK, White SH, Menon GK, Ghadially R, Elias P: Membrane structure in normal and essential fatty acid-deficient stratum corneum; characterization of ruthenium tetroxide staining and X-ray diffraction. *J Invest Dermatol* 96:215–223, 1991

Imokawa G, Abe A, Kawashima M, Hidano A: Decreased levels of ceramides in stratum corneum of atopid dermatitis: an etiologic factor in atopic dry skin? *J Invest Dermatol* 96:523–526, 1991

Lavrijsen APM, Bouwstra JA, Gooris GS, Boddé HE, Ponec M: Reduced skin barrier function parallels abnormal stratum corneum lipid organisation in patients with lamellar ichthyosis. *J Invest Dermatol* 105:619–624, 1995

Madison KC, Swartzendruber DC, Wertz PW, Downing DT: Presence of intact Intercellular lipid lamellae in the upper layers of the stratum corneum. *J Invest Dermatol* 88:714–718, 1987

McIntosh TJ, Stewart ME, Downing DT: X-ray diffraction analysis of isolated skin lipids: reconstruction of intercellular lipid domains. *Biochemistry* 35:3649–3653, 1996

Melton JL, Wertz PW, Swartzendruber DC, Downing DT: Effects of essential fatty acid deficiency on epidermal O-acylsphingolipids and transepidermal water loss in young pigs. *Biochim Biophys Acta* 921:191–197, 1987

Ohman H, Vahlquist A: *In vivo* studies concerning a pH gradient in human stratum corneum and upper epidermis. *Acta-Derm-Venereol* 74:375–379, 1994

Pilgram GSK, Engelsma-van Pelt AM, Bouwstra JA, Koerten HK: Electron diffraction provides new information on human stratum corneum lipid organization in relation to depth and temperature. *J Invest Dermatol* 113:403–409, 1999

Pilgram GSK, Vissers DCJ, van der Meulen H, Pavel S, Lavrijsen SPM, Bouwstra JA, Koerten HK: Aberrant lipid organization in stratum corneum of patients with atopic dermatitis and lamellar ichthhyosis. *J Invest Dermatol*, 2001

Ponec M, Weerheim A, Kempenaar J, Mommaas AM, Nugteren DH: Lipid composition of cultured human keratinocytes in relation to their differentiation. *J Lipid Res* 29:949–962, 1988

Robson KJ, Stewart ME, Michelsen S, Lazo ND, Downing DT: 6-Hydroxy-4-sphingenine in human epidermal ceramides. *J Lipid Res* 35:2060–2064, 1994

Sage BH, Huke RH, McFarland AC, Kowalczyk K: The importance of skin pH in iontophoresis of peptides. In: Brain K. James V, Walters KA: eds. *Prediction Percutaneous Penetration*, Cardiff: STS Publishing, 1993:pp 410–418

Schreiner V, Gooris GS, Pfeiffer S, *et al*: Barrier characteristics of different human skin types investigated with X-ray diffraction, lipid analysis and electron microscopy imaging. *J Invest Dermatol* 114:654–660, 2000

Swartzendruber DC: Studies of epidermal lipids using electron microscopy. *Seminars Dermatol* 11:157–161, 1992

Wertz PW, Downing DT: Ceramides of pig stratum epidermis, structure determination. *J Lipid Res* 24:753–758, 1983

Wertz PW, Downing DT: In: Goldsmith LA, ed. *Physiology, Biochemistry, and Molecular Biology of the Skin*, 2nd edn. Oxford University Press, 1991:pp 205–236

White SH, Mirejovsky D, King GI: Structure of lamellar lipid domains and corneocyte envelopes of murine stratum corneum. An X-ray diffraction study. *Biochemistry* 27:3725–3732, 1988